Journal of Atmospheric and Solar-Terrestrial Physics 70 (2008) 1694–1713

Contents lists available at ScienceDirect

Journal of Atmospheric and Solar-Terrestrial Physics

journal homepage: www.elsevier.com/locate/jastp

Review of modeling of losses and sources of relativistic electrons in the outer radiation belt II: Local acceleration and loss

Yuri Y. Shprits [a,*], Dmitriy A. Subbotin [a], Nigel P. Meredith [b], Scot R. Elkington [c]

[a] UCLA, Department of Atmospheric Sciences, 7127 MS, Box 951565, Los Angeles, CA 90095-1565, USA
[b] British Antarctic Survey, Natural Environment Research Council, High Cross, Madingley Road, Cambridge CB3 0ET, UK
[c] Laboratory for Atmospheric and Space Physics, University of Colorado at Boulder, 1234 Innovation Drive, Boulder, CO 80303, USA

ARTICLE INFO

Article history:
Accepted 15 June 2008
Available online 2 July 2008

Keywords:
Radiation belts
Local acceleration
Local loss
Modeling

ABSTRACT

This paper focuses on the modeling of local acceleration and loss processes in the outer radiation belt. We begin by reviewing the statistical properties of waves that violate the first and second adiabatic invariants, leading to the loss and acceleration of high energy electrons in the outer radiation belt. After a brief description of the most commonly accepted methodology for computing quasi-linear diffusion coefficients, we present pitch-angle scattering simulations by (i) plasmaspheric hiss, (ii) a combination of plasmaspheric hiss and electromagnetic ion cyclotron (EMIC) waves, (iii) chorus waves, and (iv) a combination of chorus and EMIC waves. Simulations of the local acceleration and loss processes show that statistically, the net effect of chorus waves is acceleration at MeV energies and loss at hundreds of keV energies. The combination of three-dimensional (3D) simulations of the local processes and radial transport show that the complexity of the behavior of the radiation belts is due to a number of competing processes of acceleration and loss, and depends on the dynamics of the plasmasphere, ring current, and solar wind conditions.

1. Introduction

Recent observations and theoretical studies have shown that a number of different processes determine the evolution of the radiation belt electrons at different levels of geomagnetic activity. Fig. 1 illustrates the various loss and source processes operating during geomagnetically quiet and disturbed conditions.

During geomagnetically quiet conditions, the plasmapause can move out beyond geosynchronous orbit. Resonant interactions with plasmaspheric hiss is the dominant scattering process at $L>2.5$, and provides losses on typical timescales of 5–20 days at 1 MeV (e.g., Selesnick et al., 2003; Meredith et al., 2006, 2007). At lower L-values, pitch-angle scattering is dominated by Coulomb collisions resonant interactions with lightning-generated whistlers and anthropogenic VLF transmissions (Abel and Thorne, 1998).

During geomagnetic storms, the plasmapause is eroded and compressed, and radiation belt relativistic electrons find themselves in a very different plasma environment outside the plasmasphere. Horne and Thorne (1998) and Summers et al. (1998) suggested that resonant wave-particle interactions with whistler-mode chorus waves outside the plasmasphere may result in the local acceleration of electrons. A growing number of observational studies (Green and Kivelson, 2004; Iles et al., 2006; Chen et al., 2006, 2007) and radiation belt reanalysis studies which used data assimilation tools (Koller et al., 2007; Shprits et al., 2007b) show that peaks in the phase space density of relativistic electrons build up between 4.5 and 6 R_E during relativistic electron flux enhancements in the outer radiation belt. The only possible explanation for such an evolution of the phase space density is the presence of a local source of relativistic electrons in the inner magnetosphere. Consistent with this, the build

* Corresponding author. Tel.: +1 310 8251038.
E-mail address: yshprits@atmos.ucla.edu (Y.Y. Shprits).

1364-6826/$ - see front matter
doi:10.1016/j.jastp.2008.06.014

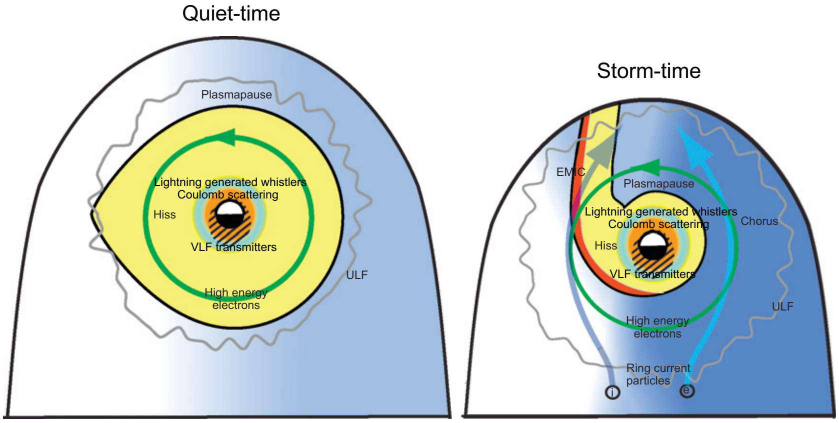

Fig. 1. Dominant acceleration and loss processes under quiet (left) and disturbed (right) geomagnetic conditions. Orange and blue circles close to the Earth depict areas where Coulomb collision scattering and scattering by lightening-generated whistlers, respectively, play important roles. The hatched area on the night-side represents scattering by VLF transmitters. The green arrow shows the circular trajectory of the relativistic electrons. Yellow indicates the location of plasmaspheric hiss inside the plasmasphere and in the region of plumes. The light blue arrow shows the trajectory of the injected ring current electrons that excite chorus waves (blue) on the dawn side, while the gray line corresponds to ring current ions exciting EMIC waves (red) on the dusk-side of the plasmasphere and in the regions of plumes. The curved line indicates ULF waves driving inward and outward radial diffusion.

up of relativistic electrons a few days into the recovery phase of storms has been found to be correlated with geomagnetic indices, enhanced fluxes of seed electrons, and enhanced chorus wave intensities (Meredith et al., 2002, 2003a). Furthermore, the statistical study of O'Brien et al. (2003) showed that electron flux enhancements across the outer radiation belt are generally related to both ULF and VLF/ELF activity.

During geomagnetic storms, electrons may also be accelerated to relativistic energies by shock-induced acceleration (Li et al., 1993, 1997; Hudson et al., 1997). Substorm activity produces a source population that may be abruptly moved by a pressure pulse into regions of stronger magnetic field, which produces rapid enhancement of the relativistic electrons in the outer zone (Ingraham et al., 2001). However, such events are rather rare and cannot explain most of the dynamic variability of the radiation belts.

Losses outside the plasmasphere are driven by pitch-angle scattering due to whistler-mode chorus waves (Horne and Thorne, 2003; O'Brien et al., 2004; Thorne et al., 2005a; Shprits et al., 2007b), and the combined effect of losses to the magnetopause followed by outward radial diffusion (Shprits et al., 2006c). Losses inside the plasmasphere are dominated by plasmaspheric hiss (Lyons et al., 1972; Lyons and Thorne, 1973; Abel and Thorne, 1998; Meredith et al., 2006, 2007) and electromagnetic ion cyclotron (EMIC) waves (Millan et al., 2002; Summers and Thorne, 2003; Meredith et al., 2003b; Albert, 2003; Bortnik et al., 2006; Li et al., 2007).

2. Pitch-angle and energy diffusion

For an electron in a magnetic field, resonant interactions occur when in the electron reference frame, multiples of gyrofrequency are equal to the wave frequency, and may be written in the lab frame as

$$\omega - k_{||}v_{||} = n\Omega_e/\gamma, \quad n = 0, \pm 1, 2, 3, \ldots, \tag{1}$$

where ω is the wave frequency, $k_{||}$ and $v_{||}$ are the components of the wave vector and electron velocity parallel to the ambient magnetic field, respectively, Ω_e is the electron gyrofrequency, and $\gamma = (1-v^2/c^2)^{-1/2}$.

During resonant wave-particle interactions, ELF and VLF waves can violate the first and second adiabatic invariants and diffuse electrons in pitch-angle and energy. Diffusion in pitch-angle transports electrons into the loss cone, where they collide with atmospheric particles and are lost from the system. Energy diffusion, which can be significant during wave-particle interactions with several types of waves, can harden the energy spectrum and accelerate electrons to MeV energies. To quantify these processes, a detailed knowledge of the amplitudes and spectral properties of the waves is required. In this section, we review the statistical properties of the ELF/VLF and EMIC waves responsible for the violation of the first and the second adiabatic invariants. Section 3 shows pitch-angle scattering simulations by various plasma waves and estimates the loss timescales associated with scattering by each type of wave, followed in Section 4 by two-dimensional (2D) simulations of scattering in pitch-angle and energy. Section 5 presents three-dimensional (3D) simulations of radial transport, local acceleration, and pitch-angle scattering. Additional local acceleration and loss mechanisms are briefly described in Section 6. Section 7 summarizes this review and outlines a roadmap for future research and model development.

2.1. *Major types of waves capable of violating the first and second adiabatic invariants*

Fig. 2 shows examples of the ELF/VLF plasma waves typically observed in the inner magnetosphere. Here, the wave electric field spectral intensity is plotted against UT for a single orbit beginning at perigee at 1742:18 UT on September 12, 1990, and ending at the next perigee at 0248:50 UT on September 13, 1990. The magnetic local